J. Phys. E: Sci. Instrum., Vol. 16, 1983. Printed in Great Britain

An on-line digital phase sensitive detector in the range 2 mHz–2 kHz

G J Gerritsma, W J van Weezep, J A Overweg and J Flokstra
Twente University of Technology, PO Box 217,
7500 AE Enschede, The Netherlands

Received 29 September 1982, in final form 8 November 1982

Abstract. A digital phase sensitive detector (PSD) has been designed and built which may be used in conjunction with a SQUID-based AC susceptibility measurement system. The system operates in a useful frequency range from 2 mHz–2 kHz and measures both the in-phase and the quadrature component.

The digital PSD, which is based on a small minicomputer, corrects for DC drift and flux quantum jumps of the SQUID and operates in 'real time'. An analysis of its design and several properties and measuring results are presented.

1. Introduction

At the ISMAR Ampère conference we presented (Overweg *et al* 1980) an AC susceptibility measurement system which is based on a commercially available SQUID and associated electronics (SHE 330). This system is used to measure the relaxation properties of magnetic materials, whereby the frequency may be swept. Its layout is shown in figure 1. The static magnetic field, produced by a 5 Tesla superconducting solenoid, is modulated with a small oscillating magnetic field produced by a primary coil system (P). The output of a secondary coil system (S) is fed into the SQUID. Part of the primary drive signal is coupled into the secondary system through a transformer (T) in order to balance the secondary circuit. The SQUID-system operates in the flux-locked mode, the feedback signal is applied to the transformer.

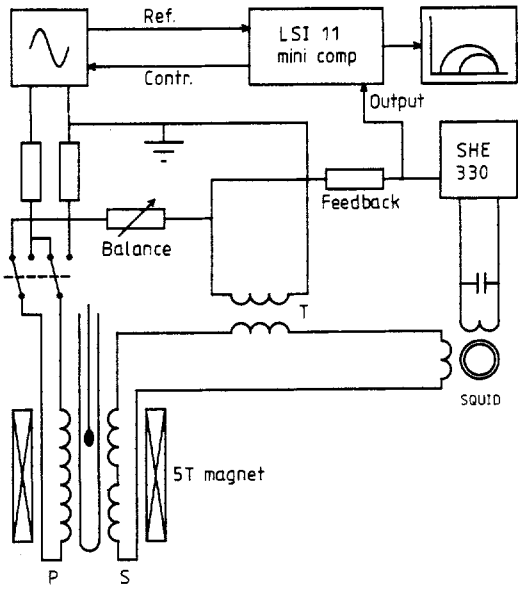

Figure 1. Schematic drawing of the AC susceptibility measuring system.

Compared to a traditional Hartshorn bridge this circuit offers two distinct advantages:

(i) The flux coupled into the SQUID is independent of the frequency of the field modulation and is converted into a voltage that is proportional to this flux.

(ii) Because of its large amplitude, the output signal produced by the SQUID electronics need not be selectively amplified before it can be fed into the actual phase detecting circuitry of an analogue PSD.

The combination of these two features allows a frequency-swept operation of the system. The bandwidth of the system is limited to the range 10 Hz–6 kHz. The upper limit is due to the phase shifts produced by the feedback electronics of the SQUID system. Low-frequency measurements are seriously hampered by drift and sudden jumps of the output signal. The former are mainly caused by temperature drift of the sample and the corresponding drift of its magnetisation, the latter by electromagnetic interference into the coil system and by resets of the SQUID electronics if the endpoints of its linear range are reached. The slow response of the analogue PSD to these disturbances is responsible for the lower limit.

In order to extend the bandwidth of our AC susceptibility measurement system down to much lower frequencies we decided to replace the analogue PSD by a digital PSD. In that case the lower frequency limit is determined by the drift of the SQUID signal and the ability of the PSD to cope with this drift. The upper frequency limit is determined by the highest rate at which the analogue signals may be sampled, digitised and processed.

In § 2 design criteria for the digital PSD are specified. In § 3 the design choices are made and possible solutions are presented. In § 4 we describe the realisation of the instrument and some important algorithms. In § 5 its transfer function is derived. Experimental results are presented in § 6 and final conclusions are given in § 7.

2. Design criteria for the PSD

The most important design criteria are related to the characteristics of the signal to be measured and to our basic experimental needs. The frequency response of the SQUID system is determined by the characteristics of the flux-locked loop (feedback loop) and is flat from DC to 20 kHz for small signals. For large signals the bandwidth is restricted by the slew rate of the flux-locked loop. We found for example in the so-called FAST-mode that the useful bandwidth was restricted to about 800 Hz. At higher frequencies the phase shift is intolerable. We made a careful analysis of the response of the system and it turned out that the frequency response of the feedback electronics of the SHE 330 is the main cause of the low bandwidth. Using the external feedback output (ext. FB) this part of the circuitry may be bypassed. This output signal was fed back into the external transformer (T) and we were thus able to increase the bandwidth to about 6 kHz with a maximum phase shift of 1.5 degrees.

Apart from the signal from the sample, a phase-shifted sine wave, unwanted components are also present. Owing to the high sensitivity of the measuring system even for DC signals, temperature drift, causing a change in the magnetisation of the sample, produces a relatively large drift. Furthermore, interference caused by other laboratory equipment may induce signals with slopes exceeding the maximum slew rate of the feedback loop. The system will then temporarily lose lock and when it relocks the baseline of the output signal has jumped to another level. Next, the signal contains the usual components of the power line frequency and its odd harmonics. All coils in the

system are made astatic and ground loops are avoided in order to reduce this interference to an acceptable level.

Besides the above mentioned signal properties, our experimental needs have to be considered. Our primary purpose was to extend the measuring range which we obtained with analogue PSDs down to much lower frequencies. A low-frequency limit of about 0.01 Hz was thought necessary in order to perform the experiments we had in mind (Overweg *et al* 1981). Although our analogue PSDs could be used down to 10 Hz accurate measurements could only be obtained at frequencies above 40 Hz. An upper limit of 100 Hz for the digital PSD was desirable and it would be nice if the digital PSD could be used up to several kHz so that we could cover the entire frequency range of the SQUID with the digital system. Both in-phase and quadrature components should be measured and recorded.

In order to speed up the measurements, a high throughput was thought necessary.

To summarise, the following design criteria are to be met:
(i) signal bandwidth 0.01 Hz–100 Hz (1 kHz preferably)
(ii) amplitude with an accuracy of 1% and phase with an accuracy of 1°
(iii) insensitivity to large linear drift of the signal
(iv) insensitivity to baseline jumps of the signal
(v) a high throughput, comparable to that of an analogue PSD.

In order to fulfil all of these criteria the digital PSD has to be designed around a mini- or microcomputer. Furthermore, the design of sophisticated specialised hardware is time consuming and would therefore not be cost effective. The computer should at least have a data acquisition unit with two analogue input channels, one for the signal and one for the reference, a programmable clock to synchronise the data sampling and a plotter interface. Apart from these minimum requirements a storage medium and a digital-to-analogue converter can be very useful, the first to store the measurements for later retrieval and the second to control the frequency of the external oscillator. In this way we are able to build an automatic frequency-swept measuring system with data storage. By storing the data, several refinements may be obtained. If no sample is placed in the measuring coil system, so-called empty-coil measurements may be performed. These data may be used to correct the data that are obtained if a particular sample is placed in the coils. Other refinements are for instance that the data be displayed in any suitable format.

3. Design of a digital PSD

If $s(t)$ is the signal and $r(t)$ the reference (sine wave or square wave) analogue phase detection is performed by forming the product $s(t)r(t)$ in a modulator followed by a low-pass filter. If the quadrature component is needed $r(t)$ is shifted over 90°. This type of phase detection can be easily incorporated into a digital system by using an analogue multiplier followed by an analogue-to-digital converter. However, this solution, although it is cost effective and guarantees high throughput, is not insensitive to linear drift and jumps. These problems may be overcome in a digital design.

Here we present several algorithms that are insensitive to linear drift and nevertheless guarantee a high throughput. The basic formula for the in-phase component IP is given by:

$$\text{IP} = \frac{c}{T}\int_0^T s(t)r(t)\,\mathrm{d}t \tag{1}$$

where T is the reference period and c the gain constant of the system. A high throughput may be obtained if we replace $r(t)$ by its square wave representation so that multiplication within the integral may be avoided. If we simplify our notation by the following definition

$$I_{4m+n} = \int_{mT+nT/4}^{mT+(n+1)T/4} s(t)\,\mathrm{d}t \qquad \begin{matrix} n=0,\,1,\,2,\,3 \text{ and} \\ m=0,\,1,\,2 \text{ etc.} \end{matrix} \tag{2}$$

the in-phase and quadrature components of the signal may by conveniently written as (unity gain)

$$\text{IP} = (I_0 + I_1 - I_2 - I_3)\pi/2T \tag{3}$$

$$\text{QP} = (I_0 - I_1 - I_2 + I_3)\pi/2T. \tag{4}$$

By substituting $s(t) = A\sin(2\pi t/T + \varphi)$ it is easy to show that $\text{IP} = A\cos\varphi$ and $\text{QP} = A\sin\varphi$. Furthermore if the signal contains a linear drift term $B + Ct$ it can be shown that the quadrature component is insensitive to this drift, whereas the in-phase component is not. This may be overcome by a simple trick, i.e. by taking

$$\text{IP} = (I_1 - I_2 - I_3 + I_4)\pi/2T \tag{5}$$

at the expense of a reduction in throughput because the measurement time is extended by one quarter period. Another solution to this problem is to integrate the signal over two periods separated by an odd number of half periods. For one half period this leads to

$$\text{IP} = (I_0 + I_1 - I_2 - I_3 - I_6 - I_7 + I_8 + I_9)\pi/4T. \tag{6}$$

In order to calculate the required integrals with a minimum of computational effort we replace them by an unweighted sum of samples, i.e.

$$I = \frac{1}{K}\sum_{k=1}^{K} s(t_k) \tag{7}$$

where $s(t_k)$ is a sample of the signal taken at time t_k and K is the number of samples within a quarter period. The factor $1/K$ before the summation is introduced to normalise the result. If we replace $s(t_k)$ by $\frac{1}{2}[s(t_k - T_c/2) + s(t_k + T_c/2)]$, where T_c is the sample clock period, it is easy to see that the summation is equivalent to the familiar trapezoid rule of numerical integration, hence

$$I = \frac{1}{KT_c}\int_{t_1 - T_c/2}^{t_K + T_c/2} s(t)\,\mathrm{d}t. \tag{8}$$

The bounds of this integral do, however, in general not coincide with those of a quarter period because the sample clock is independent of the reference signal. If we define $\delta T_1 = t_1 - T_c/2$ and $\delta T_2 = KT_c - T/4$ and use equations (3) and (4) to calculate IP and QP it may be shown that

$$\text{IP}' = A\cos(\varphi + \delta\varphi_1 + 2\delta\varphi_2)\cos^2\delta\varphi_2 \tag{9}$$

$$\text{QP}' = A\sin(\varphi + \delta\varphi_1 + 2\delta\varphi_2)\cos\delta\varphi_2(1 + \sin\delta\varphi_2) \tag{10}$$

where IP′ and QP′ are the new, but incorrect phase components, $\delta\varphi_1 = 2\pi\delta T_1/T$ and $\delta\varphi_2 = 2\pi\delta T_2/T$. From this we may conclude that two types of error are introduced by this simple numerical integration technique. The first is caused by the term δT_1 and introduces a phase shift, whereas the second caused by δT_2 'detunes' the phase detector giving rise to a phase shift and an amplitude error. In order to keep these phase shifts within 1° the sample clock frequency should be at least about a thousand times higher than the signal frequency. This restriction seriously limits the high frequency limit of the PSD. Both errors may be reduced, however, if more signal periods are taken into account. The term δT_2 may be calculated with any required accuracy if we measure the ratio T/T_c by counting the number of sample clock periods within a sufficiently large number of signal periods and T_c is accurately known. Using equations (9) and (10) this

error may then be corrected and only the unknown phase shift $\delta\varphi_1$ remains. This term may effectively be reduced if we calculate IP and QP from an average over several not necessarily adjacent, periods. If we assume that $KT_c \neq T/4$ and take the periodic nature of the signal into account, then averaging over M periods is equivalent to taking $4KM$ samples of the signal in a given period which are more or less uniformly distributed over the interval. This reduces the effective phase error to $|\delta\varphi_1/M| \leqslant \pi T_c/MT$ and in the extreme case that $T_c \sim T/4$, i.e. one sample per quarter period, only 45 periods are needed to reduce this phase shift to 1°. The error introduced by δT_2 may also be reduced if the computer is able to tune T_c or T in such a way that T_c/T approximates, but is not equal to a multiple of 4. The restriction 'is not equal to' is necessary in order to reduce the phase shift $\delta\varphi_1$.

The next phenomena we have to take care of are the baseline jumps of $s(t)$. At low frequencies a correction may be made by comparing two successive samples $s(t)$ and $s(t+T_c)$ of the signal. If the difference $s(t+T_c)-s(t)$ exceeds $2\pi AT_c/T$ we know that this cannot arise from the signal $s(t)=A\sin(2\pi t/T+\varphi)$ alone. In those cases we take $s(t+T_c)=s(t)$ and make a real time baseline correction to the digitised signal.

This correction is not perfect as it also includes a legitimate difference between successive samples. In practice, we take a somewhat higher jump criterion because of noise, hum and possible quantisation errors. If the signal period is no longer large compared to the sample period IP and QP are determined by averaging over several periods. If the mean time interval between successive baseline jumps is larger than this measurement time at least some of the measurements, if we repeat this procedure several times, should produce correct results and the others, in which a jump occured, deviate substantially from those. Using a 'cluster technique' we are able to distinguish between correct and incorrect results. The way this is done is best illustrated with an example given in table 1.

Table 1.

	Measurement number			
$tol^2=25$	1	2	3	4
IP	13	14	10	40
QP	16	12	15	25
$dist^2$	—	1^2+4^2	3^2+1^2	27^2+9^2
$dist^2$	1^2+4^2	—	4^2+3^2	26^2+13^2
$dist^2$	3^2+1^2	4^2+3^2	—	30^2+10^2
$dist^2$	27^2+9^2	26^2+13^2	30^2+10^2	—
$n$hits	2	2	2	0

On the first line of this table four measurements of IP are presented and on the next line the corresponding values of QP. On the next four lines a matrix of squared distances is given. The entries in this matrix are calculated from the expression $(IP_i-IP_j)^2+(QP_i-QP_j)^2$ where the indices i and j refer to distinct measurements. As a next step these entries are compared column by column with the square of a given tolerance (here $tol^2=25$). The number of hits, i.e. the number of times the squared distance is less than or equal to the squared tolerance, is recorded on the last line. In the given example the measurements 1, 2 and 3 lie in a cluster whereas measurement 4 does not. If for one of the columns $n$hits $\geqslant n$limit the procedure may be stopped, for we then know that at least $n$limit + 1 measurements agree and we also know which ones. The parameter $n$limit is set to an acceptable value. The in-phase and quadrature components are then given by the average of those corresponding measurements. If $n$hits $< n$limit extra measurements are added until $n$hits $\geqslant n$limit. Some precautions have to be taken that guarantee that this procedure does not continue for ever. Furthermore, the tolerance has to be chosen carefully, otherwise incorrect results are obtained.

4. Realisation of a digital PSD

In the preceding section we presented several algorithms which can be used as building blocks for a digital PSD having the required properties. To implement the PSD we used an LSI 11/2 minicomputer with 56 kbytes of memory, a terminal, a dual double density floppy disc and a 16 bits parallel input/output unit. Coupled to this unit is a homemade interface system with a bus structure. Into this interface system up to 16 peripheral units may be plugged. The basic peripheral units we used to implement the PSD are an ADAC unit, a programmable clock unit and a plotter interface unit. In the ADAC unit we used a Data Translation DT 5702 with an eight-channel differential multiplexer, a differential amplifier, a sample and hold amplifier and a 12 bits analogue-to-digital converter. Furthermore the unit contains a 12 bits digital-to-analogue converter. The programmable clock has a basic 1 MHz oscillator, followed by a programmable interval timer (Intel 8253). A square wave may be generated by this unit with a period that is a multiple of 1 μs. The plotter interface unit is used to drive ordinary laboratory XY-recorders. A schematic drawing of the experimental set-up is given in figure 2.

Using this equipment, which was already present, the implementation of a PSD was a matter of software development. In the preceding section we have seen that the usefulness of the basic algorithms depends on the signal frequency. In order to make an optimal use of these algorithms we decided to divide the programs into three groups. One group for low frequencies (0.002–0.3 Hz), one for medium frequencies (0.3–10 Hz) and one for high frequencies (10 Hz–2 kHz).

The communication between the user, the system programs and devices and the interface system is organised through a main program written in FORTRAN. If speed of operation or device programming is not prohibitive this language is used, otherwise we used the assembly language MACRO. The user may for instance instruct the program to start a frequency sweep from a lower bound to an upper bound in a given number of discrete steps and to plot the measuring results in an Argand diagram (figure 5(*a*)). Furthermore, several parameters have to be specified by the user, the most important ones being the tolerance (tol) that is used in the cluster technique, the noise level that may be expected in order to make an appropriate correction for baseline jumps, an effective integration time constant and some scaling factors. In order to obtain one measurement of IP and QP the main program calls another program that either estimates or measures the reference frequency. Depending on this particular frequency the low-, medium- or high-frequency program groups are selected to perform the actual measurement of IP and QP.

In the low-frequency region equations (4) and (5) are used to obtain IP and QP and baseline jumps are corrected on a real time basis. The sample clock period T_c is adjusted in such a way that about 20 000 samples per period may be expected. First an offset is determined by performing several measurements of a short-circuited analogue input channel. This is necessary in order to detect the zero crossings in case a sine wave reference is used. For a square wave reference this offset is less important. Next the reference period is measured, followed by the calculation of five partial sums of the signal.
The period measuring algorithm is as follows:

$$pos:=neg:=false;\ N:=0;\ nr:=2;$$

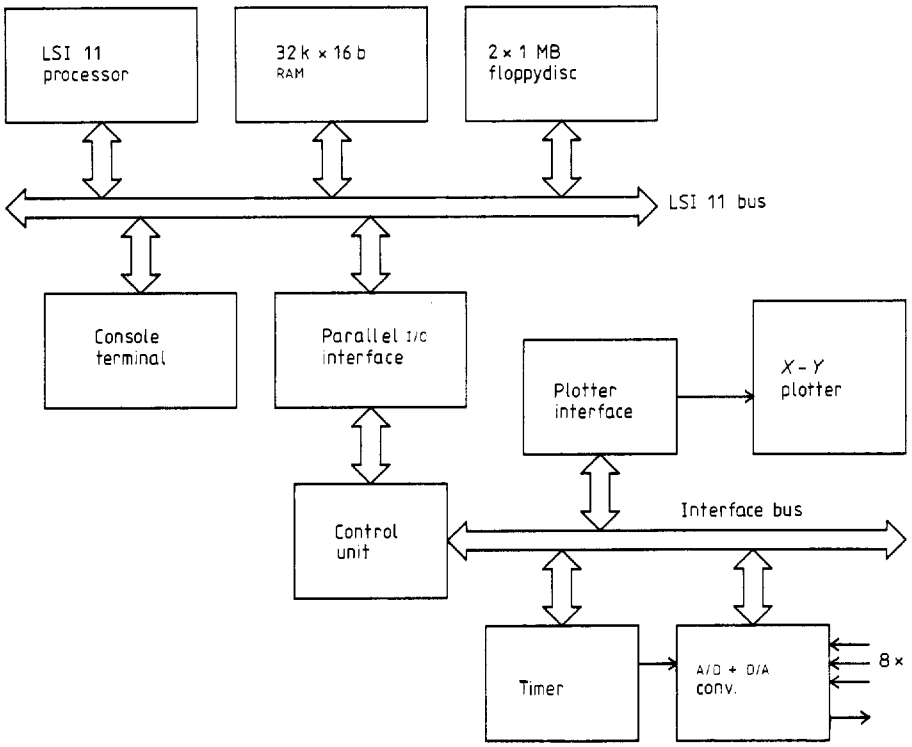

Figure 2. The digital phase sensitive detector based on a LSI 11/2 processor and a homemade interface system.

```
zeroed: if sample (ref) > offset
        then if neg = true then goto pslope else pos := true
        else if pos = true then goto nslope else neg := true;
        goto zeroed;

pslope: N := N + 1;
        if sample (ref) < offset
        then begin nr := nr − 1;
        if nr = 0 then goto integration else goto nslope
        end
        else goto pslope;

nslope: N := N + 1;
        if sample (ref) ⩾ offset
        then begin nr := nr − 1;
        if nr = 0 then goto integration else goto pslope
        end
        else goto nslope;

integration: comment the number of samples per period N is now
known;
```

From this point on an integration algorithm is entered, which per quarter period including baseline jump correction is as follows:

```
accu := 0;

for i := 1 step 1 until N ÷ 4 do
begin s := sample (sig);
      difference := previous difference − s;
      if abs (difference) ⩾ jump then offset := offset − difference;
      previous difference := s;
      s := s − offset;
      accu := accu + s;

      end;
```

The procedure 'sample' produces a sample of the channel specified in its parameter list, synchronous with the clock.

This algorithm is repeated five times and each partial sum is stored in a different accumulator (accu). The accumulated results are used to calculate IP and QP. Although the foregoing algorithms are written in ALGOL for the sake of clarity the actual algorithms are written in the assembly language MACRO to improve speed. All variables used are one-word integers, except accu which is a double-word integer.

In the medium-frequency region equations (4) and (5) are used to obtain IP and QP. Baseline jumps are corrected for on a real time basis but the cluster technique is also used in order to obtain reliable results. The reference period T is measured by counting the number of samples that may be taken within several periods. Next, the programmable clock is tuned in such a way that T is almost a multiple of $4T_c$. The measurements are continued until at least five of them agree according to the cluster technique. If this does not happen within twenty measurements the tolerance is doubled, redoubled etc. until at least three measurements agree. This procedure ensures that the measurements do not continue indefinitely. The resulting averaged IP and QP are next corrected for two errors. The first is a phase delay error caused by the properties of our ADAC unit. A zero crossing of the reference is detected if two consecutive samples differ in sign. In § 3 it was assumed that the sampling process of the signal channel could be started right after the zero crossing of the reference. However, our ADAC unit does not have separate sample and hold amplifiers for reference channel and signal channel. The required signal sample can thus not be taken. Furthermore the multiplexer has to be switched from the reference channel to the signal channel at the cost of an extra sample period. The first signal sample that is available to the LSI 11/2 is two clock cycles later. However, the phase shift is accurately known as $\delta\varphi_1 = 4\pi T_c/T$ and may be corrected for afterwards. The next error that occurs is the one caused by the difference $\delta T_2 = KT_c - T/4$ and this may also be corrected for if T is accurately known.

In the high-frequency region real time baseline jump

corrections are no longer possible and only the cluster technique remains. The sample clock period is adjusted to the shortest possible value (about 80 μs), but may after the determination of T be increased in 1 μs steps in order to make δT_2 almost equal to zero. Equation (6) is used to obtain IP and an equivalent equation for QP. The MACRO routine accumulates IP and QP over approximately 200 ms, giving an effective integration time constant of 1 s if the first five measurements all belong to the same cluster. This time constant may be selected during the measurements.

5. Selectivity of the digital PSD

In order to obtain insight into the behaviour of this digital PSD as a measuring instrument we will now derive a power transfer function for a rather general algorithm. We assume that IP and QP are obtained from a measurement that integrates over n_1 consecutive periods, waits n_2 periods and repeats this process n_3 times (n_1 and n_3 are integer and n_2 is half integer).

We define a complex transfer function for the in-phase component of the signal as

$$\bar{F}_I(\omega)=\frac{\pi}{2iT}\frac{1}{n_3}\sum_{k=0}^{n_3-1}\exp\{ik[\omega(n_1+n_2)T+\pi]\}\times\frac{1}{n_1}\sum_{l=0}^{n_1-1}\exp(il\omega T)\times\left(\int_0^{T/2}\exp[i(\omega t+\varphi)]\,dt-\int_{T/2}^{T}\exp[i(\omega t+\varphi)]\,dt\right). \quad (11)$$

In the same way we define a complex transfer function for the quadrature component of the signal $\bar{F}_Q(\omega)$ which has a modified term inside the square brackets. It is easy to see that both $\bar{F}_I(\omega)$ and $\bar{F}_Q(\omega)$ are proportional to $\exp(i\varphi)$, but otherwise they are a complicated complex function of ω, T, n_1, n_2 and n_3. Note that ω is now the signal frequency while T is the reference period and $\omega_0=2\pi/T$ is in general not equal to ω. In order to simplify the expressions we define a power transfer function $F^2=\bar{F}\bar{F}^*$ where $\bar{F}^*$ is the complex conjugate of $\bar{F}$. Furthermore, we are not interested in both phase components separately, although there are some differences, so we will take the average of both power transfer functions.

After some algebra we get

$$F^2(x)=\left(\frac{\sqrt{2}}{x}\sin\frac{\pi x}{2}\sin\frac{\pi x}{4}\right)^2\left(\frac{1}{n_1}\frac{\sin n_1\pi x}{\sin\pi x}\right)^2\times\left(\frac{1}{n_3}\frac{\sin n_3((n_1+n_2)\pi x+\pi/2)}{\sin((n_1+n_2)\pi x+\pi/2)}\right)^2 \quad (12)$$

where $x=\omega/\omega_0$ and henceforth the successive terms in large round brackets are denoted by $I(x)$, $II(x)$ and $III(x)$. In figures 3–4 this function is plotted for some values of n_1, n_2 and n_3 as a function of ω/ω_0.

First of all, it may be noted that peaks occur at ω_0, $3\omega_0$, $5\omega_0$, etc, which may be expected because we have in fact multiplied the signal $s(t)$ with a square wave reference signal $r(t)$, instead of a sine wave. Secondly we note that extra peaks occur in the spectra and thirdly we have an indication from these figures that the bandwidth (SBW) and perhaps the noise bandwidth (NBW) decrease with increasing total measurement time.

In order to obtain more rigorous results about SBW and NBW we deduced these quantities in the approximate manner as follows.

If $n_1=n_3=1$ then $II(x)=III(x)=1$ and hence the power transfer function is equal to $I^2(x)$. This function has zeros if x is even and for x is odd it takes on the values given by $I^2(x)=1/x^2$. The SBW may be found by replacing x by $1+\Delta x$ and expanding $I(x)$ up to second order in Δx. If we then solve the quadratic equation $I(\Delta x)=1/\sqrt{2}$ we obtain the approximate results SBW = 0.94 which is not very much different from the value found by a straightforward numerical solution to the problem giving SBW = 0.97. In order to calculate NBW we make a change of variables by substituting $\xi=\pi x/4$ and using some goniometric rules we obtain

$$I^2(\xi)=\frac{\pi^2}{2}\left[\frac{\sin^4\xi}{\xi^2}-\frac{\sin^6\xi}{\xi^2}\right]. \quad (13)$$

This function may be integrated by using a set of indefinite integrals given on page 188 of a table of integrals (Gradsteyn and Ryzhik 1965).

$$\int\frac{\sin^{2m}x}{x^2}\,dx=-\binom{2m}{m}\frac{1}{2^{2m}x}+\frac{(-1)}{2^{2m-1}}\sum_{k=0}^{m-1}(-1)^{k-1}\binom{2m}{k}\times\{\cos[(2m-2k)x]/x+(2m-2k)\,\mathrm{si}[(2m-2k)x]\} \quad (14)$$

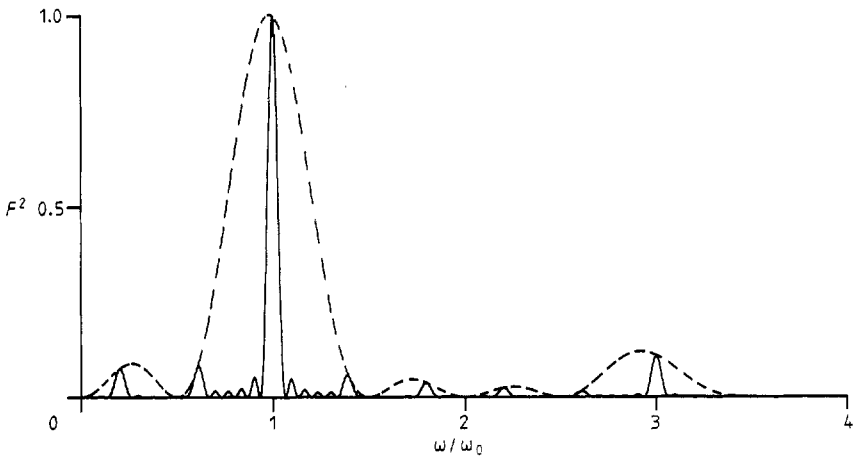

Figure 3. Power transfer function of a digital PSD for $n_1=2$, $n_2=0.5$ and $n_3=6$ (full curve) and $n_1=2$, $n_2=0.5$ and $n_3=1$ (broken curve)

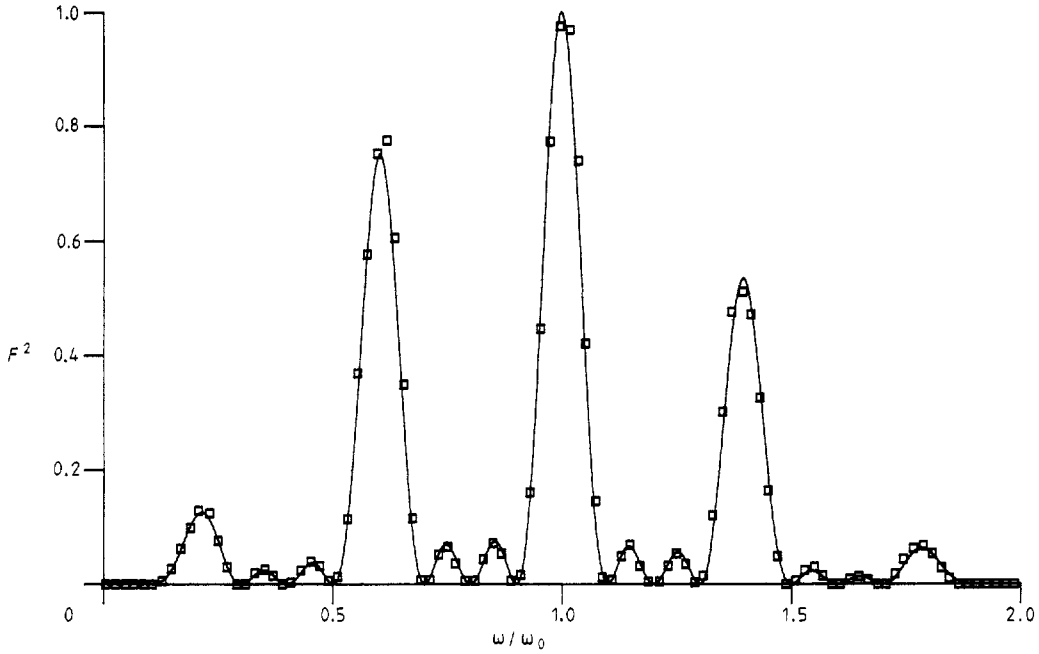

Figure 4. Calculated power transfer function of a digital PSD for $n_1 = 1$, $n_2 = 1.5$ and $n_3 = 4$ (full curve) compared with measured function (symbols).

where $\mathrm{si}(x) = \mathrm{Si}(x) - \pi/2$

and $\mathrm{Si}(x) = \int_0^x \frac{\sin t}{t}\,\mathrm{d}t.$

For $m = 2$ and $x \to 0$ this integral is equal to $-\pi/4$ and in case $m = 3$ it is equal to $-3\pi/16$. For large values of x the function $\mathrm{si}(x)$ may be approximated by $-\cos x/x$. Combining these we obtain

$$\int_0^x I^2(\xi)\,\mathrm{d}\xi = \frac{\pi^2}{2}\left[\left(\frac{\pi}{4} - \frac{3}{8x}\right) - \left(\frac{3\pi}{16} - \frac{10}{32x}\right)\right]$$

$$= \frac{\pi^2}{32}\left(\pi - \frac{1}{x}\right). \tag{15}$$

If we compare this approximate result with results obtained by numerical integration we find that for $x \geqslant \pi/2$ the error in the approximation is less than 2% and hence

$$\mathrm{NBW} \sim \frac{4}{\pi}\,\frac{\pi^3}{32} = \frac{\pi^2}{8}.$$

Furthermore, we are interested in the average values $\bar{I}^2(\xi)$ in the regions between successive zeros of this function. If we relate these average values to the values of $\hat{I}^2(\xi)$ in the middle of the regions, i.e. for $x = 1, 3, 5$, etc, we find using equation (15) that $\bar{I}^2(\xi)/\hat{I}^2(\xi) \sim \frac{1}{2}$ (accurate to within 20%).

As a next step, we analyse the second part of the power transfer functions $II^2(x)$. It has zeros for $x = k/n_1$ with $k = 0, 1, 2$, etc, except when $x = 0, 1, 2$, etc, when the function has peaks of height one. The peaks for even values of x are suppressed by the zeros of $I^2(x)$. The SBW may be found by replacing x by $1 + \Delta x$ and expanding the nominator up to third order in Δx. For large values of n_1 we may then replace the sine in the denominator by its argument and hence we obtain

$$II(x) \sim 1 - \tfrac{1}{6}(n_1 \pi\,\Delta x)^2. \tag{16}$$

From this approximation we obtain $\mathrm{SBW} = 0.84/n_1$. Improved results may be obtained by numerical calculation of SBW for different values of n_1. From this we obtain an improved approximation $\mathrm{SBW} = 0.9/n_1$ which has an error less than 10% for $n_1 \geqslant 2$.

Combining $I(x)$ and $II(x)$ and following an analogous procedure it can be shown that the previous result for SBW may be extended to $n_1 \geqslant 1$ with the same error margin.

In order to obtain the NBW we use a set of definite integrals given on page 371 of a table of integrals (Gradsteyn and Ryzhik 1965).

$$\int_0^{\pi/2} \left(\frac{\sin ax}{\sin x}\right)^2 \mathrm{d}x = a\,\frac{\pi}{2}. \tag{17}$$

The NBW for the case $n_3 = 1$, but $n_1 \geqslant 2$ may be obtained as follows

$$\mathrm{NBW} = \sum_{k=1}^{\infty} \int_{2(k-1)}^{2k} I^2(x) II^2(x)\,\mathrm{d}x \sim \sum_{k=1}^{\infty} \bar{I}^2(x = 2k-1) \times \int_{2(k-1)}^{2k} II^2(x)\,\mathrm{d}x \tag{18}$$

$$\mathrm{NBW} \sim \sum_{k=1}^{\infty} \frac{1}{2}\,\hat{I}^2(x = 2k-1) \int_0^2 II^2(x)\,\mathrm{d}x = \sum_{k=1}^{\infty} \frac{1}{2(2k-1)^2} \cdot \frac{2}{n_1} \tag{19}$$

$$\mathrm{NBW} \sim \frac{1}{n_1}\left(\sum_{k=1}^{\infty} \frac{1}{k^2} - \frac{1}{4}\sum_{k=1}^{\infty} \frac{1}{k^2}\right) = \frac{\pi^2}{8n_1}. \tag{20}$$

Comparing this with the previous results for $n_1 = n_3 = 1$ we see that equation 20 remains valid for $n_1 = 1$.

As $III^2(x)$ behaves in the same manner as $II^2(x)$ we find for the noise bandwidth

$$\mathrm{NBW} = \sum_{k=1}^{\infty} \int_{2(k-1)}^{2k} I^2(x) II^2(x) III^2(x)\,\mathrm{d}x \sim \sum_{k=1}^{\infty} \overline{I^2(x_k) II^2(x_k)} \int_0^2 III^2(x)\,\mathrm{d}x \tag{21}$$

and hence

$$\text{NBW} = \frac{\pi^2}{16 n_1} \int_0^2 III^2(x)\, dx = \frac{\pi^2}{8 n_1 n_3}. \qquad (22)$$

The signal bandwidth may again be obtained by replacing x by $1 + \Delta x$ and expanding the function into powers of Δx. From this we obtain the approximate result $\text{NBW} \sim 0.84/n_3(n_1 + n_2)$ $(n_3 \geqslant 2)$ which may be improved to $\text{NBW} \sim 0.9/n_3(n_1 + n_2)$ by comparison with numerical results.

We may thus conclude this analysis by the following results. The signal bandwidth is given by

$$\text{SBW} = \frac{0.9}{n_3(n_1 + n_2)} \ (n_3 \geqslant 2) \ \text{ or } \ \frac{0.9}{n_1} \ (n_3 = 1) \qquad (23)$$

Comparison with numerical calculation shows that the error is $<10\%$ for $n_1 = n_3 = 1$ and $<2\%$ in all other cases.

The noise bandwidth is given by equation (22) and the error is $<3\%$. The SWB is hence inversely proportional to the total time the measurement takes, i.e. $n_3(n_1 + n_2)T$ whereas NBW is inversely proportional to the total time the signal is actively sampled, i.e. $n_1 n_3 T$. The time the signal is not actively sampled, i.e. $n_3 n_2 T$, does not count in the NBW. Furthermore, we note that increasing n_2 reduces SBW, but introduces extra peaks in the power spectrum such that NBW is not affected.

To minimise the number of extra peaks in the power spectrum thereby reducing interference with the line power frequency $n_2 = 0.5$ is chosen in our algorithms. If we compare the preceding results with an analysis of a microcomputer based PSD that is based on a much simpler algorithm (Momo *et al* 1981) we note that the SBW is equal but the rejection of unwanted frequencies and the NBW are superior.

The power transfer function just described does not take into account the process of (re)locking to the reference each time an integration over n_1 periods starts. If this integration is performed over an interval of length $T + \Delta T$ instead of T it may be shown that the complex transfer function for the in-phase component at ω_0 is given by

$$\bar{F}_I(\omega_0) = \frac{1}{n_1} \exp(i n_1 \omega_0 \Delta T/2) \frac{\sin(n_1 \omega_0 \Delta T/2)}{\sin(\omega_0 \Delta T/2)} \times \frac{1 + \cos(\omega_0 \Delta T/2)}{2(1 + \Delta T/2)} \exp(i\varphi)$$

From this equation it may be seen that, apart from an influence on the amplitude, a phase shift of $n_1 \omega_0 \Delta T/2$ occurs. The smaller this term, the better the results are. Therefore we used $n_1 = 1$ in our algorithms. With $n_1 = 1$ and $n_2 = 0.5$ we find $\text{NBW/SBW} \sim 2$.

6. Measurements

In this section we present some of the measurements we performed with the digital PSD described in the previous sections. In figure 4 a power transfer function is given for a particular set of coefficients n_1, n_2 and n_3. The full curve is the calculated function according to equation (12). The symbols represent the measurements where for each point the average over 100 values of $\text{IP}^2 + \text{QP}^2$ is taken. The agreement between theory and experiment is excellent.

Next we performed several experiments in order to find out the useful frequency range of the instrument. As signal we used a sine wave in phase with a square wave reference, both from the same oscillator. The lowest frequency turned out to be about 0.002 Hz. This is determined by the lowest sample clock period of 32 ms and the largest signed number of the computer (32000) and may be easily extended downwards. The highest frequency is about 3 kHz and is determined by the highest sample clock frequency of about 12 kHz. It is the limit given by the fact that at least one sample per quarter period has to be taken. The bottleneck lies in the number of instructions to implement the basic algorithms and the speed of the LSI 11/2 processor. The sample clock frequency may be increased if the data are sampled and stored but not operated upon in 'real time'. This may lead to an improvement by a factor of four and then the bottleneck lies in the ADAC unit. In the range 10 Hz–2 kHz we found that with a few exceptions the measured in-phase component was constant and the absolute value of the quadrature component less than 1.3% of the in-phase component. This corresponds to a maximum absolute phase error of 0.75 degrees, well within the design limits.

Finally we present in figure 5 some measurements of a 5% chromium aluminium potassium alum sample, where the complete experimental set-up was used, including the SQUID detector. For a given temperature and static magnetic field the dynamic susceptibility was measured in the range 1 Hz–1 kHz. The in-phase component (dispersion) and quadrature component (absorption) are given in the form of an Argand diagram in figure 5(*a*) together with the empty-coil effect. Each frequency decade contains 20 points and the total measurement time is about 7 min, i.e. for each point approximately 7 s are needed. The effective integration time constant chosen for this particular experiment was 1 s. This is comparable to the speed at which an analogue PSD with the same time constant could perform the measurements with the same accuracy, i.e. about 5 s for a 1% accuracy. In figure 5(*b*) the measurements on the sample are presented, but now corrected for the empty-coil effect. The corrected measurements lie almost on two semi circles in good agreement with theory.

In another experiment we isolated the sample as well as possible from the helium bath. Within several hours its temperature rose from 4.2 K (the temperature of the bath) to 10 K. This temperature drift induced a large drift in the signal and hundreds of resets occured giving rise to baseline jumps larger than the harmonic signal. Nevertheless, many frequency sweeps were made each sweep taking about 7 min. The performance of the digital PSD was, however, hardly influenced by these extremely bad conditions and reasonable Argand diagrams were obtained.

7. Conclusions

In this paper we showed how to design a digital PSD based on a minicomputer. The system has a useful range of 2 mHz–2 kHz where, except for some frequencies that cause interference with the line power frequency, the phase error never exceeds 1°. The instrument has now been in use for about two years and fully met all its design criteria. The fact that a frequency sweep can be made in about 7 min, except for the lowest frequencies, is a considerable improvement compared to previous measurement techniques. Furthermore, it is now possible to perform relaxation experiments at phase transitions which show narrow peaks in the susceptibility against the magnetic field. The static magnetic field may be adjusted accurately on a given position of such peaks whereas in the traditional technique of measuring AC susceptibilities the magnetic field is swept.

Using the basic concepts that are described in this paper, many variations may be made on the digital PSD that is represented here. During the two years of its operation we made several changes to improve both the performance of the digital PSD and the performance of the measurement system as a whole. A major example of the first category is a change of the MACRO routine that accumulates IP and QP in the low-frequency range in order to optimise it for the shortest possible overall measurement time. In order to achieve this, the accumulation process already starts, together with the measurement of the period, immediately after the first zero crossing of $r(t)$ has been

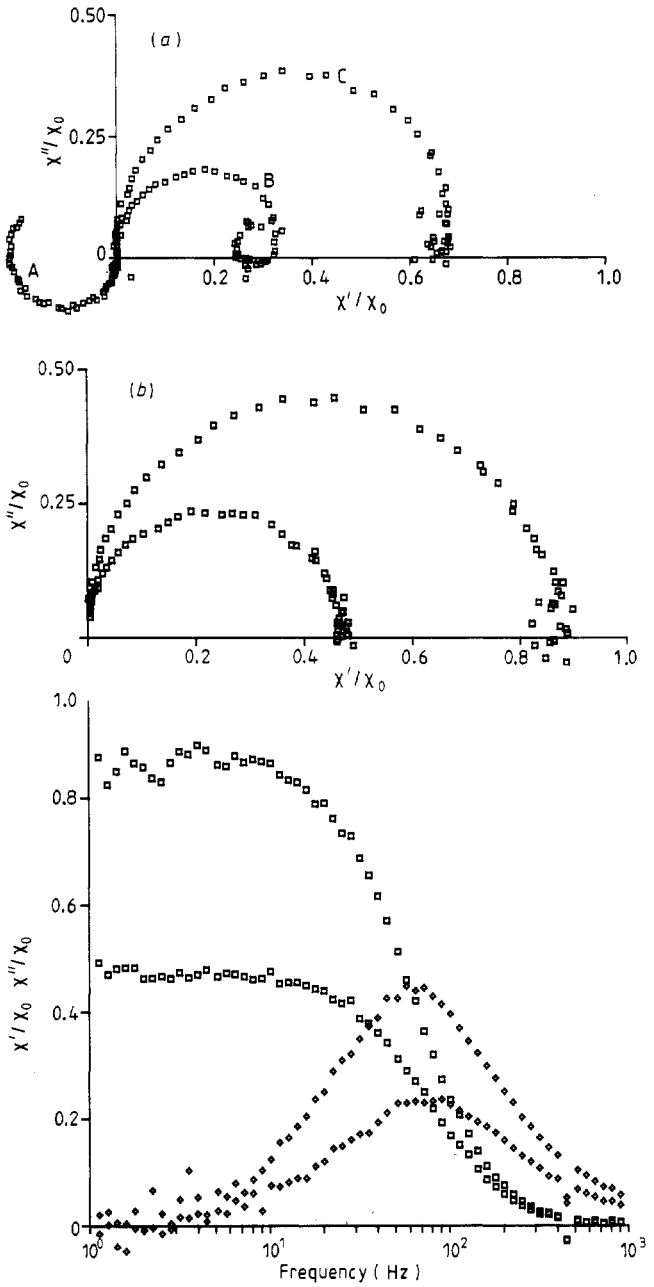

Figure 5. (*a*) Argand diagram of 5% chromium aluminium potassium alum sample at 3.2 K and 0.92 T. χ' = dispersion (in-phase component), χ'' = absorption (quadrature component) and χ_0 = zero-field susceptibility. A, empty-coil effect; B, vacuum curve; and C, saturated vapour curve. (*b*), The same as (*a*) but now corrected for the empty-coil effect and also dispersion and absorption against frequency.

detected. The accumulation time is first calculated from an estimated frequency of the computer driven external oscillator; when after half a period this initial guess is found to deviate more than 5% from the actual frequency, the accumulation is restarted. After five quarter periods IP and QP are calculated and a FORTRAN routine then corrects for the detuning error, caused by the difference between estimated and mesaured frequency. A major example of the second category is the use of an analogue PSD as well. This extends the frequency range of the system to higher frequencies (6 kHz) and improves the throughput at frequencies >100 Hz.

References

Gradsteyn I S and Ryzhik I M 1965 *Table of Integrals, Series and Products* (New York and London: Academic)

Momo F, Ranieri G A, Sotgiu A and Terenzi M 1981 Microcomputer based phase sensitive detector *J. Phys. E: Sci. Instrum.* **14** 1253–6

Overweg J A, Flokstra J and Gerritsma G J 1980 A SQUID based frequency sweeping system for AC-susceptibility measurements *Proc. ISMAR Ampère, Delft* (Philadelphia: The Franklin Institute) 433–6

Overweg J A, Flokstra J, ter Brake J H M and Gerritsma G J 1981 Partial lattice participation in the spin-lattice relaxation of potassium chromium alum *Physica* **107B** + **C** 363–4